Comparative analysis of the neurochemical profile and MAO inhibition properties of N-(furan-2-ylmethyl)-N-methylprop-2-yn-1-amine

Philippe De Deurwaerdère,[a] Claudia Binda,[b] Rémi Corne,[a] Cosima Leone,[c] Aurora Valeri,[d] Massimo Valoti,[c] Rona R. Ramsay,[e]Yagamare Fall,[f] and José Marco-Contelles[g,*]

[a]Centre National de la Recherche Scientifique, Institut des Maladies Neurodégénératives, UMR CNRS 5293, Bordeaux (France)

[b]Dipartimento di Biologia e Biotecnologie, Università di Pavia (Italy)

[c]Dipartimento di Scienze della Vita, Università di Siena (Italy)

[d]Dipartimento di Chimica, Biologia e Biotecnologia, Università di Perugia (Italy)

[e]Biomedical Sciences Research Complex, University of St Andrews (UK)

[f]Departamento de Química Orgánica, Universidad de Vigo (Spain)

[g]Laboratory of Medicinal Chemistry (IQOG, CSIC), Madrid (Spain)

KEYWORDS: Propargylamines; crystallography; monoamine neurochemistry; neuroprotection; Alzheimer's disease; enzymology

ABBREVIATIONS: aCSF, artificial cerebrospinal fluid; AD, Alzheimer's disease; COMT, catechol-*O*-methyl transferase; CYP, cytochrome P450; DA, dopamine; DOPAC, 3,4-dihydroxyphenylacetic acid; F2MPA, *N*-(furan-2-ylmethyl)-*N*-methylprop-2-yn-1-amine; 5-HIAA, 5-hydroxyindoleacetic acid; hMAO, human monoamine oxidase; 5-HT, serotonin; HVA, homovanillic acid; MAO, monoamine oxidase; MAOI, monoamine oxidase inhibitor; 3-MT, 3-methoxytyramine; NE, noradrenaline.

Corresponding Author

José Marco-Contelles

Laboratory of Medicinal Chemistry (IQOG, CSIC), Madrid (Spain); iqoc21@iqog.csic.es

Abstract

The regulation of brain monoamine levels is paramount for cognitive functions and the enzymes monoamine oxidases (MAO A and B) play a central role in these processes. The aim of this study was to evaluate whether the pro-cognitive properties exerted by propargylamine *N*-(furan-2-ylmethyl)-*N*-methylprop-2-yn-1-amine (F2MPA) were related to changes in monoamine content via MAO inhibition. *In vivo* microdialysis and *ex vivo* amine metabolite measurement demonstrated region-specific alterations in monoamine metabolism that differ from both the classic MAO A or MAO B inhibitors clorgyline and L-deprenyl, respectively. Although all the inhibitors (1 and 4 mg/kg) increased cortical serotonin tissue content, only F2MPA increased the levels of cortical noradrenaline. In the striatum, clorgyline (1 mg/kg), but not F2MPA (1 mg/kg), reduced extracellular levels of dopamine metabolites at rest or stimulated by the intrastriatal application of the MAO substrate 3-methoxytyramin. *In vitro*, F2MPA exhibited a low affinity toward MAO B and MAO A. Nonetheless, it modified the B form of MAO, forming a flavin adduct structurally similar to that with deprenyl. F2MPA was rapidly metabolized in the presence of rat, but not human, microsomes, producing a hydroxylated derivative. In conclusion, the effect of F2MPA on cognition may arise from monoaminergic changes in the cortex, but the role of MAO in this process is likely to be negligible, consistently to the F2MPA poor affinity for MAO.

Graphical Abstract

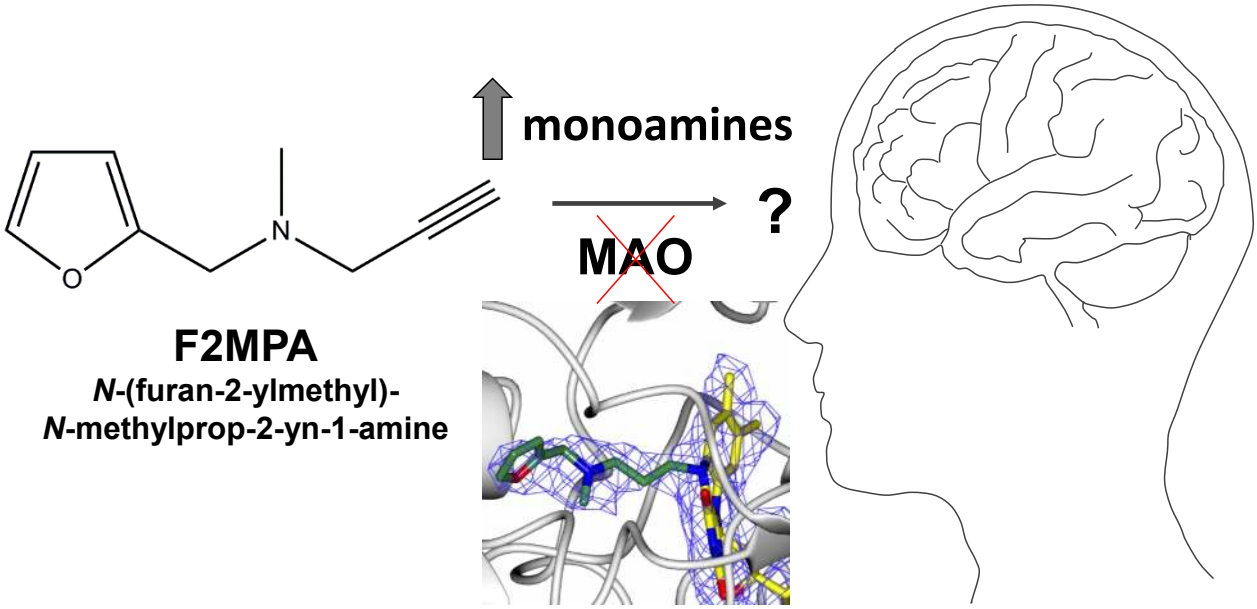

1. Introduction

The monoamine neurotransmitters dopamine (DA), adrenaline, noradrenaline (NA) and serotonin (5-HT) are aromatic molecules released by neurons in the central nervous system (CNS) to regulate cognitive processes [1], though they also have roles in peripheral tissues [2]. These neuroactive amines are paramount in mood control, behavior, emotional life, memory and many other cognitive processes in the adult brain. Impairment in metabolism and regulation of neurotransmitters may lead to serious diseases whose complexity reflects the multi-faceted functions of these endogenous compounds [3]. Among these pathological conditions, Alzheimer's disease (AD) and other dementias are increasing in the ageing populations and their economical and social impact is becoming a worrisome burden [4]. Besides aggregation of misfolded proteins and general neuronal depletion, oxidative stress is being investigated as one of the factors contributing to AD development, although antioxidant therapies have proved unsuccessful so far [5]. In this context, the comprehension of the molecular basis of AD is crucial to define the underlying neurodegenerative mechanisms and to develop new drugs. In addition to acetylcholinesterase, human monoamine oxidases A and B (hMAO A and hMAO B) are considered as possible AD targets to preserve neurotransmitters. The inhibitors of MAO also reduce the oxidative stress of hydrogen peroxide produced during the catalyzed reaction and, moreover, some of the propargyl compounds exert a neuroprotective effect by other mechanisms [6-7]. MAOs are mitochondrial membrane proteins that regulate the levels of monoamine neurotransmitters in both CNS and peripheral tissues by oxidizing the substrate amino group through the enzyme-bound FAD cofactor, which is then reoxidized by molecular oxygen with the release of hydrogen peroxide [8].

(Please insert Figure 1 here)

A number of MAO inhibitors (MAOIs) have been developed, but only a few of them are currently used in the clinical practice, mainly to treat Parkinson's disease and some types of depression [9-10]. Although encoded by different genes [11], MAO A and MAO B feature partly overlapping substrate specificity as well as similar biochemical and structural properties. Therefore, selectively targeting one of the two isozymes or even identifying the individual involvement of each in a particular process or disease is a difficult task. Historically, MAO A and MAO B are specifically inhibited by clorgyline and deprenyl, respectively, both being propargyl amines which irreversibly and covalently inactivate the enzymes. In 2014, we reported a new inhibitor of this class, *N*-(furan-2-ylmethyl)-*N*-methylprop-2-yn-1-amine (F2MPA, Figure 1), which showed enhancement of basic synaptic transmission in the hippocampus of rats [12]. In that report, F2MPA had a striking effect on the rat dentate gyrus electrophysiology, similar to that of the long-lasting potentiation effect of NE. It was suggested that it might be a promising candidate for new therapies to improve cognitive conditions in AD patients. Both the theoretical calculations and its *in vivo* efficacy at 1 mg/kg indicated that F2MPA may feature a good profile as a CNS drug. We speculated that, although the initial tests showed a low affinity of F2MPA toward MAOs, the *in vivo* effects of F2MPA could be related to a modification of monoamine function through the inhibition of MAO activities.

In the present study, we carried out a multi-approach study to investigate MAO inhibition by F2MPA and to correlate it to the effects on monoamine levels in the brain. We performed

enzymatic assays and structural analyses that confirmed F2MPA as an irreversible MAO B-specific inhibitor, but comparative *ex vivo* and microdialysis experiments suggested that the effects of F2MPA *in vivo* are likely to be unrelated to its MAO inhibitory properties.

Results and Discussion

Comparative analysis of F2MPA effect on monoamine levels in rats

Tissue measurement experiments in rats were carried out to evaluate and compare the effects of F2MPA and the classical MAOI clorgyline and deprenyl on tissue levels of monoamines and metabolites in the striatum, the cortex and the hippocampus. Based on the previous study reporting a strong effect of F2MPA at 1 mg/kg [12], we selected the doses of 1 and 4 mg/g for all drugs (Table 1). Although all compounds significantly enhanced 5-HT content in the cortex, the main result is that all compounds exhibited a distinct profile on monoamine tissue content. Deprenyl did not produce any other alteration on monoamine tissue contents at these doses whatever the region. Conversely, clorgyline significantly enhanced striatal DA levels (an effect mainly observed at the dose of 4 mg/kg) while decreasing DOPAC levels and, to a lower extent, also homovanillic acid HVA whatever the dose administered. These dopaminergic effects were not observed in the cortex. In the hippocampus, clorgyline decreased 5-HIAA tissue levels and tended, though not significantly, to increase 5-HT. Like deprenyl, clorgyline did not alter NE content whatever the regions.

The data with clorgyline recall that MAO A is mainly involved in the regulation of the dopaminergic system in the striatum [13-18], but, elsewhere, its role in the metabolism of DA and of 5-HT is region-dependent [8, 16]. The lack of effect of clorgyline on NE tissue content is not surprising because it usually requires higher non-selective doses or chronic treatment to have a pronounced effect. Although both MAO isoforms are present in all brain regions [19-21], a general, less pronounced effect of deprenyl with respect to clorgyline was confirmed [8, 16]. It should be noted that, apart from its presence in serotonergic neurons, MAO B is present mainly in glial cells and astrocytes, whereas MAO A is predominantly expressed in all neurons with the exception of serotonergic neurons [19-20].

Although the tissue data confirmed that F2MPA is already efficacious at 1 mg/kg [12], its neurochemical profile on monoamines did not correspond to the neuropharmacological signature of either a MAO A or a MAO B inhibitor. Indeed, at variance with clorgyline, it did not alter the dopaminergic metabolism in the striatum. Rather, F2MPA slightly decreased striatal DA only at the dose of 1 mg/kg without altering DOPAC content, and it increased HVA at the dose of 4 mg/kg. Although we could not measure DA in the cortex in this experiment due to unexpected loss of sensitivity, we found that F2MPA increased NE content specifically in the cortex. In contrast to its excitatory effect on 5-HT content in the cortex, F2MPA reduced striatal 5-HT content and its metabolite as well. In some cases, F2MPA altered the monoamine or metabolite levels less at the higher dose, in particular as regard the enhancement of 5-HT tissue levels in the cortex.

(Please insert Figure 2 here)

To better investigate an interaction of F2MPA on both resting and stimulated MAO function, we focused on the extracellular levels of HVA, one end product of MAO activity [22]. A new pharmacological approach was carried out using intracerebral reverse microdialysis. Exogenous 3-methoxytyramin (3-MT, derived endogenously from dopamine through COMT activity) was applied into the striatum of rats at increasing concentrations and extracellular levels of HVA were monitored along the experiment. We choose 3-MT over the infusion of neurotransmitters themselves to monitor the activity of MAO because the metabolic link between MAO and HVA involves two enzymatic steps, like 5-HT and 5-HIAA, but it recruits two parallel circuits in case of DA and HVA [22,23]. Moreover, while 3-MT would generate few off targets on its own [23], biogenic amines would have produced a number of other effects related to their receptors, transporters, and enzymes that would have profoundly alter local cell activities and impaired the interpretation of the data regarding MAO activity. The effect of clorgyline and F2MPA on basal and 3-MT-stimulated extracellular levels of HVA in the striatum are reported in Figure 2. As expected, 3-MT application induced a concentration-dependent increase in HVA extracellular levels in the striatum reaching approximately 150, 240 and 740% of baseline values when applied at 1, 10 and 100µM, respectively. The application of 3-MT did not alter DOPAC or 5-HIAA extracellular levels whatever the applied concentration (data not shown). The systemic injection of 1 mg/kg clorgyline significantly reduced the increase in HVA extracellular levels induced by the application of 3-MT. Significant effects were observed for all concentrations of applied 3-MT (two-way ANOVA, $F(1,17)$ with $p<0.05$ for each time point from the 30-minute time-point until the end of the monitoring). The reduction of the effect of 3-MT by clorgyline was more important at the lower concentrations of 3-MT and partial (almost 50% blockade) at

the highest concentration. The trend toward a reduction of HVA levels with clorgyline was significant with respect to control group 90 min after its administration during 45 min. We performed a separate comparison between the control group and the group treated with clorgyline because this statistical profile was dependent on the context of the four groups. Clorgyline per se inhibited HVA extracellular levels, the values being significantly lower compared to the control groups 1 h after its administration till the end of the monitoring. It is noteworthy that clorgyline also significantly reduced DOPAC and 5-HIAA extracellular levels (Student's t-test; data not shown). Conversely, F2MPA did not modify the increase in HVA extracellular levels induced by the application of 3-MT (two-way ANOVA, $F(1,19)$ with $p>0.05$ for the 12 time points of the time course; Figure 3, right panel). A separate statistical analysis between the control group and the F2MPA group also confirmed that F2MPA did not modify basal extracellular levels of HVA (Figure 2), DOPAC or 5-HIAA (ns, Student's t-test; data not shown).

Intracerebral microdialysis is a much more sensitive approach for the study of MAO A function compared to tissue measurement as exemplified in this study with clorgyline. The finding that F2MPA altered neither basal nor 3-MT-stimulated extracellular levels of HVA in contrast to clorgyline suggests that the effects reported previously *in vivo* [12] or in this study *ex vivo* are unrelated to MAO inhibition. Nonetheless, MAOIs administered acutely have complex and regional effects on monoamine content [13]. Their monoaminergic effects can result from the blockade of MAO activity, which itself differ within the various brain regions and monoaminergic systems [13, 22]. In addition, their primary effects could be modulated by complex monoaminergic interactions that are still difficult to decipher in some cases [24,25]. For instance,

the enhancement of cortical 5-HT by both MAOI could dampen the enhancement of striatal and/or hippocampal 5-HT via long loops involving the raphe nuclei[26]. The effects of MAO inhibitors are also strictly dependent on the reversible or irreversible nature of their mode of binding to MAO enzymes, so we addressed this aspect *in vitro* for F2MPA.

Characterization of hMAO A and hMAO B inhibition by F2MPA

To probe hMAO inhibition by F2MPA, the fluorometric horseradish peroxidase-coupled assay described in the method was used to determine IC_{50} values for initial binding, which were 214 ± 17 µM for hMAO A and 111 ± 4 µM for hMAO B. To test for irreversible inhibition after pre-incubation, the IC_{50} was also determined after 30 min preincubation at 30°C. For hMAO A, the IC_{50} was 232 ± 15 µM, not significantly different from the value measured without incubation, suggesting that hMAO A is not irreversibly inactivated by F2MPA. In contrast, the IC_{50} for MAO B after 30 min preincubation was 8.9 ± 1.2 µM suggesting that hMAO B was irreversibly inactivated after pre-incubation with F2MPA in a time- and concentration-dependent manner. These results prompted further experiments to determine the inactivation rate parameters by the Kitz and Wilson method [27-28] as shown in **Table 2**. hMAO B inactivation by F2MPA gave a K_I value of 135 ± 23 µM and k_{inact} of 0.61 ± 0.09 min^{-1}. For comparison, the typical MAO B inactivator, deprenyl, gave a K_I of 0.18 ± 0.01 µM and k_{inact} of 1.06 ± 0.03 min^{-1}. For hMAO B, the specificity constant (k_{inact}/K_I) shows that FMPA is three orders of magnitude less effective than deprenyl. The detailed investigation also revealed that, with high concentrations and longer times, MAO A was also inactivated although the rate constant was seven times slower (k_{inact} = 0.087 min^{-1}) than for MAO B. That FMPA is four orders of magnitude less effective than the

MAO A-selective inactivator, clorgyline, is clear from the specificity constant which is 5 min^{-1} μM^{-1} for clorgyline but only 0.0005 min^{-1} μM^{-1} for FMPA on MAO A (**Table 2**).

As the formation of the covalent adduct occurred over a time range of minutes, we were able to measure by the spectrophotometric assay, the reversible inhibition of hMAO B by F2MPA. F2MPA competitively inhibits hMAO B with a K_i of 317 ± 86 µM. This and the high IC50 values without preincubation indicate that the affinity for reversible binding to either hMAO A or B is very low, suggesting that inactivation of hMAO B *in vivo* may be difficult to achieve (while almost impossible for hMAO A with its very slow k_{inact}).

(Please insert Figure 3 here - structure)

The structure of the F2MPA-MAO B adduct

Inspection of the UV-visible spectrum of F2MPA-inactivated MAO B showed the same modified flavin peak (data not shown) encountered with other propargyl inhibitors such as deprenyl [29-30], which suggested that F2MPA may form a similar covalent adduct with the hMAO B cofactor. The crystal structure of hMAO B in complex with F2MPA was solved at 2.4 Å. The electron density map of the inhibitor is continuous with that of the FAD cofactor, indicating that the flavin N5 atom reacted with the propargyl unit of the compound forming a covalent adduct (Figure 3A) which resembles those found for all the other inhibitors of this class [30]. Although F2MPA is identically bound in either of the two protein molecules that occupy the asymmetric unit (rmsd = 0.27 Å), the adduct is slightly better defined in subunit B and we will refer to it for the

following discussion. The furan ring of F2MPA lies in the rear of the substrate cavity with the gating Ile199 side chain adopting the open conformation. Some degree of ambiguity exists in the exact position of the furan oxygen atom because the ring could rotate 180° along the axis of the propargyl side chain. On the basis of the electron density it is not possible to discriminate between the two possibilities and in either case the oxygen would not be at H-bond distance with any residue to predict one conformation as the most favorable. In the final refined structure, the inhibitor was modelled with the furan oxygen pointing towards the bottom of the cavity, as this portion of the active site is occupied by water molecules and, therefore, is presumably less hydrophobic. However, it cannot be ruled out that the furan ring may freely rotate without adopting a fixed unique conformation. The F2MPA molecule is in van der Waals contact with the enzyme active site residues (Figure 3B), whose conformation is the same as that found in other hMAO B structures. The position of the three solvent molecules at the bottom of the substrate cavity in front of the flavin is also conserved as is the water molecule that mediates the H-bond interaction between Lys296 and the flavin N5 atom. Superposition of the hMAO B-pargyline structure (PDB code 1GOS) onto the enzyme in complex with F2MPA revealed a high similarity (Figure 3B), in particular in the position of the acetylenic atoms. In addition, the N-CH_3 group adopts a similar conformation with the methyl group pointing towards Tyr435, whereas the furan ring is oriented in the same plane as the aromatic moiety of pargyline. The F2MPA adduct is very well conserved also with respect to the hMAO B-deprenyl structure (PDB code 2BYB), with the main difference existing in the position of the aromatic ring of deprenyl that, because its acetylenic chain is longer, lies further to the rear of the active site cavity (Figure 3C). The hMAO B crystal structure showed that F2MPA forms a covalent adduct

highly similar to that found by other propargyl inhibitors including deprenyl (Figure 3C), which implies that, once bound to the active site, F2MPA inactivates the enzyme as stably as deprenyl.

Metabolic stability of F2MPA

The discrepancy of the effects *in vivo* from that expected for a MAO B-specific inactivating inhibitor led us to investigate whether *in vivo* metabolism of F2MPA could be occurring. The metabolic stability of F2MPA was assessed upon incubation with human or rat liver microsomal preparations. The plot of the natural logarithm of the non-metabolized compound (%) versus time was linear (Figure 4), indicating that the substrate depletion followed a monoexponential relationship. With human liver microsomes, the calculated rate constant (k) for the decay was 0.002156 min^{-1}, which corresponds to a half-life time of $t_{½}$ 321 min, and the resulting Cl_{int} was 5.39 µL/min per mg of protein. In contrast, rat microsomes were able to metabolize the compound at very high rate, with a $t_{½}$ of only 10.0 min and an intrinsic clearance of 182 µL/min per mg protein.

The MS analysis of the incubation mixture of rat microsomes revealed the presence of a metabolite at $[M+16]^+$ (*m/z*) identified as a derivative hydroxylated, probably on the position 6 on the furan ring according with MetaSite in silico analysis [31]. Conversely, the incubation of F2MPA (up to 50 µM) with human microsomes did not reveal any metabolite(s) produced by cytochromes P450 (CYP). These results clearly indicate that F2MPA is not a substrate of any human liver CYPs (or a very poor one), whereas it features a very low metabolic stability in rats. These divergent behaviors between human and rat have to be considered for the interpretation

of the *ex vivo/in vivo* described above. In the rat studies, F2MPA is rapidly metabolised and, although the hydroxylated derivative of F2MPA may still inhibit MAO B, the fact that the cognitive-enhancing properties of the inhibitor appear to be MAO-independent suggests that this metabolite might act also on other targets.

Conclusions

A combination of neurochemical, metabolic and biochemical studies were performed to dissect the MAO inhibitory properties of F2MPA, a propargyl-containing compound that was previously highlighted for its cognitive-enhancing effects (Figure 1; Di Giovanni et al., 2014). The main result of this study is that tissue measurement experiments showed that F2MPA produces changes in rat brain monoamine levels, such as a combined increase in 5-HT and NE levels in the cortex, which are distinct from those induced by the typical MAO inhibitors clorgyline and deprenyl. The dissimilarity is consistent with the weak inhibition properties of F2MPA with respect to both isozymes (IC50 values are 214 µM and 111 µM for human MAO A and MAO B, respectively). The crystal structure of human MAO B in complex with F2MPA revealed that the inhibitor does form a covalent adduct with the enzyme flavin cofactor similarly to other acetylenic compounds such as deprenyl and rasagiline. However, irreversible inactivation of MAO B gave a K_I value of 193 µM and k_{inact} of 0.252 min^{-1}, indicating that F2MPA is much weaker than deprenyl but similarly fast in forming the covalent adduct with FAD observed in the crystal structure. Metabolic stability investigations showed some discrepancies between human and rat systems, with the latter featuring a CYP-dependent formation of a F2MPA metabolite that is not observed in humans. As binding affinity values were measured with rat MAOs which are similar

to those found for the human enzymes (Table 2), it can be concluded that the pro-cognitive profile of F2MPA described earlier [12] could be related to a still unknown action on monoamine systems, which is independent from its very poor MAO inhibition properties. A full pharmacological description of its binding profile on various receptors, enzymes and transporters is still not available, impairing any further comments on its mechanism of action.

Methods

Chemicals and reagents

Deprenyl hydrochloride, clorgyline hydrochloride, 3-methoxytyramine (3-MT) hydrochloride as well as all compounds for neurochemistry (dopamine hydrochloride, noradrenaline hydrochloride, serotonin hydrochloride, 3,4-dihydroxyphenylacetic acid (DOPAC), homovanillic acid (HVA), or 5-hydroxyindolacetic acid, 5-HIAA) and other reagents were purchased from Sigma-Aldrich. F2MPA was synthesized as before [12]. Compounds were dissolved in sterile NaCl 0.9% for their systemic injection in animals.

Animals

Experiments were performed on 79 male Sprague-Dawley rats (Charles River, L'Arbresle Cedex, France) weighing 250-300 g on arrival, housed under a 12:12 h light:dark cycle with food and water *ad libitum*. All experiments involving animals are reported in accordance with the ARRIVE guidelines (see legends to figures). Protocols were approved by the Ethical Committee of Centre National de la Recherche Scientifique, Région Aquitaine-Limousin (Agreements n°50120166-A and 50120126-A). All experiments conformed to European Economic Community (86-6091 EEC)

and French National Committee (*décret* 87/848, Ministère de l'Agriculture et de la Forêt) guidelines for the care and use of laboratory animals. All procedures were as humane as possible and efforts were made to reduce the number of animals used.

Microdialysis

Rats were anaesthetized with isoflurane (3%) in a plastic chamber as previously described [32]. Animals were then fixed on a stereotaxic apparatus with a nose mask adapted to it to allow continuous delivery of the anesthetic gas during probe implantation and microdialysis experiment (isoflurane, 1.5%). A feedback-controlled heating pad was employed to keep body temperature at 37 °C. The tip of the microdialysis probe (4 mm length, CMA/11, 240 µm outer diameter; Phymep, France) was implanted in the striatum as follow: AP = 9.7; L = 3; V = 2.4 with respect to the interaural point [33]. Perfusion of the microdialysis probe with the artificial cerebrospinal fluid (aCSF) (154.1 mM Cl^-, 147 mM Na^+, 2.7 mM K^+, 1 mM Mg^{2+} and 1.2 mM Ca^{2+} adjusted to pH 7.4 with 2 mM sodium phosphate buffer) was performed at a constant flow rate (2 µl/min) with a microperfusion pump (CMA 100, Phymep, France). Two hours after implantation (a timeframe corresponding to steady-state [34], dialysates were collected every 15 min and stored on ice. At the end of the experiment, anesthetized rats were sacrificed for histological verification of the correct placement of the microdialysis probe.

Chromatographic analyses

Tissue concentration of monoamines and their metabolites in the striatum, the cortex and the hippocampus was measured by reverse-phase high performance liquid chromatography coupled with electrochemical detection (HPLC-ECD). Tissues were homogenized in 100 µl of 0.1 N $HClO_4$ and then centrifuged (13,000 rpm, 30 min, 4 °C). Aliquots (10 µl) of the supernatants were injected into the HPLC column (Chromasyl C8, 150 X 4.6 mm, 5 µm) protected by a Brownlee-Newgard precolumn (RP-8, 15 x 3.2 mm, 7 µm). The mobile phase (60 mM NaH_2PO_4 , 0.1 mM disodium EDTA, 2 mM octane sulfonic acid with 7% methanol, with the addition of orthophosphoric acid to adjust pH at 3.9) was delivered at 1.2 ml/min flow rate. Detection of compounds was performed with a coulometric detector (CoulochemII, ESA) coupled to a dual-electrode analytic cell (model 5011). Electrodes were set at +350 and -270 mV potential. Results were expressed as picograms per milligram of tissue, with each value corresponding to the mean ± the standard error of the mean (s.e.m.).

Each dialysate sample (30 µl) was analyzed by HPLC-ECD as described previously [32, 34]. The mobile phase (70 mM NaH_2PO_4, 0.1 mM EDTA, 0.1 mM octylsulfonic acid with 10% methanol, with the addition of orthophosphoric acid to adjust pH at 4.5) was delivered by an Equisyl-BDS column (C18; 4.6 X 150 mm; particle size 5 µm; CIL-Cluzeau, Sainte-Foy La Grande, France) at 1 ml/min flow rate (Beckman pump 116). Detection of DOPAC, HVA and 5-HIAA was performed with an amperometric cell Ag/AgCl (VT-03) coupled to a detector (Decade II Antec, AlphaMos, Toulouse, France). Electrodes were set at +600 mV potential and output signals were recorded (Beckman, system GOLD).

Pharmacological treatments

For *post-mortem* studies, rats were habituated for one week to the room in which they received the MAOI clorgyline, deprenyl or F2MPA. On the day of the experiment, rats were given intraperitoneally 1 or 4 mg/kg of MAOI or the vehicle (sterile NaCl 0.9%) randomly between 10 and 12 am. Rats were sacrificed 3 h after the injection. The brains were quickly removed, frozen in cold isopentane (-35 °C), and kept at -80 °C pending the dissection of structures of interest (striatum, frontal cortex, hippocampus) and the biochemical analysis. In dialysis experiments, the pharmacological treatments started after the stabilization of HVA extracellular levels in the dialysates. 3-MT, dissolved in aCSF, was applied through the microdialysis probe at increasing concentrations (1, 10 and 100 µM) for 1 h each using a three-way liquid switch system (CMA111, Phymep). Control groups underwent the same procedures but syringes contained only aCSF. MAOIs (clorgyline or F2MPA) were administered intraperitoneally at 1 mg/kg 15 min before the first application of 3-MT or aCSF. Vehicle groups received the inhibitor solvent (sterile NaCl 0.9% in all cases).

Inhibition studies

Both hMAO A and hMAO B were produced as recombinant enzymes using yeast expression systems and purified as previously described [29-30]. Spectrophotometric and fluorimetric methods were used for enzymatic assays on both hMAO A and hMAO B to characterize F2MPA inhibition properties. First, using the coupled fluorescence assay and membrane-bound human MAO A or B, IC_{50} values were determined from initial rates (i.e. without pre-incubation) in the presence of

tyramine (0.8 mM for MAO A and 0.32 mM for MAO B) corresponding to about 2xK_m, using Graphpad PRISM 4 to fit the data to a three-parameter curve:

Y=Bottom + (Top-Bottom)/(1+10^(X-LogIC50)

Where the full curve was not defined, the bottom was set to zero. The results provided the proper experimental conditions for pre-incubation assays to test F2MPA for irreversible inhibition and to determine the inactivation rate (k_{inact}) and inhibition constant (K_I) [27-28]. As described previously [30], enzyme and inhibitor were incubated at 30 °C in 50 mM potassium phosphate pH 7.4 for various times before two-fold dilution by adding 1 mM tyramine and the reaction mixture containing horseradish peroxidase (HRP, 1 unit/ml final) and Ampliflu Red (20 µM final) to measure the remaining enzyme activity with respect to the control (i.e. no inhibitor). The inactivation of MAO A by clorgyline was too fast and too high affinity for this method, so MAO A was preincubated in 50 µL in a quartz cuvette before addition of 450 µL of 50 mM potassium phosphate pH 7.5 at 30°C containing 300 µM kynuramine (10x K_M) to dilute the clorgyline and measure the remaining active enzyme. Rates (as relative fluorescence units per second or as absorbance change per minute) were normalized to the initial activity and plotted as the natural log (ln) of the fractional remaining activity against time. Rates (as relative fluorescence units per second, rfu/s) were normalized to the control and plotted as the log of the fractional remaining activity against time. The rates (k_{obs}) plotted against F2MPA concentration gave a rectangular hyperbola that was fitted by non-linear analysis using the equation:

($Y = k_{inact}*X/(K_I + X)$)

For rat tissue experiments, inactivation parameters (k_{inact} and K_I) were determined as described previously [28, 30]. Rat liver homogenate was prepared from frozen rat liver at 1g in 5 mL of 50 mM potassium phosphate, pH 7.5, containing 0.2% Triton X-100. Assays contained the equivalent of 0.5 mg/ml of wet tissue.

In addition, the reversible inhibition of purified hMAO B by F2MPA was assessed in the absorbance assay using the substrates kynuramine (hMAO A) and benzylamine (hMAO B) at pH 7.5 as previously published [35].

X-ray crystallography

Crystals of hMAO B were grown following published procedures [30] using enzyme incubated with 1 mM F2MPA for 1 h (15-fold excess with respect to protein concentration). X-ray diffraction data were collected at the X06SA beamline of SLS synchrotron (Villigen, Switzerland), which were processed by MOSFLM [36] and CCP4 programs [37]. Model building by Coot [38] and refinement by Refmac5 [39] were carried out using standard protocols [30]. Statistics are reported in Table 3 and figures were produced using CCP4mg [40].

Analysis of *in vitro* metabolism of F2MPA in rat and human liver microsomes

F2MPA, dissolved in water, was incubated separately at 10 µM concentration in 100 mM phosphate buffer (pH 7.4) with 0.48 mg/mL human or rat hepatic microsomal protein as previously reported [41]. The enzymatic reactions were initiated by addition of a NADPH regenerating system consisting of 2 mM ß-nicotinamide adenine dinucleotide phosphate (NADPH), 10 mM glucose-6-phosphate (G6P), 0.4 U/ml glucose-6-phosphate dehydrogenase

(G6PDH). Reactions were terminated at regular time intervals (overall range 0-60 min) by adding a double volume of acetonitrile. All incubations were performed in triplicate. Samples were analyzed by mass spectrometry using an Agilent 6540 UHD Accurate-Mass Q-TOF LC/MS spectrometer operated in positive electrospray mode. The experimental data obtained were analyzed using Mass-MetaSite, a computer assisted method for the interpretation of LC–MSMS data that combines prediction of the Site of Metabolism (SoM) of the compound with the processing of MS spectra and rationalization based on fragment analysis [42]. The intrinsic clearance (Cl_{int}) was calculated by the equation:

$Cl_{int} = k(min-1)x\ [V]/[P]$

where k is the rate constant for the depletion of substrate, V is the volume of incubation in µL and P is the amount of microsomal proteins in the incubation medium in mg [43].

Statistics

The effect of MAOIs on tissue levels of monoamines and metabolites was analysed by a one-way ANOVA using the dose (0, 1 or 4mg/kg) as the main factor for each compound. In case of significance ($p<0.05$), it was followed by the protected least significant difference test (PLSD test) to allow for multiple comparisons between groups. The effect of clorgyline or F2MPA on basal and stimulated extracellular levels of HVA was analysed by a two-way ANOVA for each time point of the time course using the factors MAOI X 3-MT. In case of significance, indicating that the effect of the treatment 3-MT is modified by the MAOI, this first analysis was followed by a one-way ANOVA with group as the main factor in order to perform the post hoc PLSD test for multiple comparisons between groups. We also performed separate analysis using repeated

measures to determine the own effect of the two MAOIs on basal extracellular levels. In all cases, $p<0.05$ was the criterion for statistical significance.

Funding Sources

Collaborations among authors were enabled by COST Action CM1103, *Structure-based drug design for diagnosis and treatment of neurological diseases.* CB thanks Fondazione Cariplo (project n. 2014-0672) and the BioStruct-X program (project n. 10205) for funding synchrotron trips. PDD thanks the support of Idex Bordeaux (PEPS IDEX project 2013).

Acknowledgements

CB thanks the Swiss Light Source (SLS) for providing beamtime and assistance. The participation of Hasna El Boukhari, Anouk Pierre and Nouhad Samb to the microdialysis/tissue measurement experiments is gratefully acknowledged. PDD acknowledges the Centre National de la Recherche Scientifique.

Author contributions

JMC and YG designed and synthesized molecule F2MPA. PDD, CB, MV and RRR designed the experiments. PDD, CB, RC, CL, AV, MV, and RRR contributed to the experimental manipulations and analyzed the data. PDD, CB, MV, RRR and JMC wrote the article.

Disclosures

The authors declare no financial conflict of interest.

References

1. Haavik, J.; Blau, N.; Thony, B., Mutations in human monoamine-related neurotransmitter pathway genes. *Human mutation* **2008,** *29* (7), 891-902.
2. Mialet-Perez, J.; Bianchi, P.; Kunduzova, O.; Parini, A., New insights on receptor-dependent and monoamine oxidase-dependent effects of serotonin in the heart. *Journal of neural transmission (Vienna, Austria : 1996)* **2007,** *114* (6), 823-7.
3. Ng, J.; Papandreou, A.; Heales, S. J.; Kurian, M. A., Monoamine neurotransmitter disorders--clinical advances and future perspectives. *Nature reviews. Neurology* **2015,** *11* (10), 567-84.
4. Rafii, M. S.; Aisen, P. S., Advances in Alzheimer's disease drug development. *BMC medicine* **2015,** *13*, 62.
5. Rosini, M.; Simoni, E.; Milelli, A.; Minarini, A.; Melchiorre, C., Oxidative stress in Alzheimer's disease: are we connecting the dots? *Journal of medicinal chemistry* **2014,** *57* (7), 2821-31.
6. Naoi, M.; Maruyama, W.; Inaba-Hasegawa, K., Revelation in the neuroprotective functions of rasagiline and selegiline: the induction of distinct genes by different mechanisms. *Expert review of neurotherapeutics* **2013,** *13* (6), 671-84.
7. Wu, Y.; Kazumura, K.; Maruyama, W.; Osawa, T.; Naoi, M., Rasagiline and selegiline suppress calcium efflux from mitochondria by PK11195-induced opening of mitochondrial permeability transition pore: a novel anti-apoptotic function for neuroprotection. *Journal of neural transmission (Vienna, Austria : 1996)* **2015,** *122* (10), 1399-407.
8. Youdim, M. B.; Edmondson, D.; Tipton, K. F., The therapeutic potential of monoamine oxidase inhibitors. *Nature reviews. Neuroscience* **2006,** *7* (4), 295-309.
9. Binda, C.; Milczek, E. M.; Bonivento, D.; Wang, J.; Mattevi, A.; Edmondson, D. E., Lights and shadows on monoamine oxidase inhibition in neuroprotective pharmacological therapies. *Current topics in medicinal chemistry* **2011,** *11* (22), 2788-96.
10. Connolly, B. S.; Lang, A. E., Pharmacological treatment of Parkinson disease: a review. *Jama* **2014,** *311* (16), 1670-83.
11. Bach, A. W.; Lan, N. C.; Johnson, D. L.; Abell, C. W.; Bembenek, M. E.; Kwan, S. W.; Seeburg, P. H.; Shih, J. C., cDNA cloning of human liver monoamine oxidase A and B: molecular basis of differences in enzymatic properties. *Proceedings of the National Academy of Sciences of the United States of America* **1988,** *85* (13), 4934-8.
12. Di Giovanni, G.; Garcia, I.; Colangeli, R.; Pierucci, M.; Rivadulla, M. L.; Soriano, E.; Chioua, M.; Della Corte, L.; Yanez, M.; De Deurwaerdere, P.; Fall, Y.; Marco-Contelles, J., N-(furan-2-ylmethyl)-N-methylprop-2-yn-1-amine (F2MPA): A potential cognitive enhancer with MAO inhibitor properties. *CNS neuroscience & therapeutics* **2014,** *20* (7), 633-40.
13. Finberg, J. P., Update on the pharmacology of selective inhibitors of MAO-A and MAO-B: focus on modulation of CNS monoamine neurotransmitter release. *Pharmacology & therapeutics* **2014,** *143* (2), 133-52.
14. Brannan, T.; Prikhojan, A.; Martinez-Tica, J.; Yahr, M. D., In vivo comparison of the effects of inhibition of MAO-A versus MAO-B on striatal L-DOPA and dopamine metabolism. *Journal of neural transmission. Parkinson's disease and dementia section* **1995,** *10* (2-3), 79-89.
15. Kato, T.; Dong, B.; Ishii, K.; Kinemuchi, H., Brain dialysis: in vivo metabolism of dopamine and serotonin by monoamine oxidase A but not B in the striatum of unrestrained rats. *Journal of neurochemistry* **1986,** *46* (4), 1277-82.
16. Kumagae, Y.; Matsui, Y.; Iwata, N., Deamination of norepinephrine, dopamine, and serotonin by type A monoamine oxidase in discrete regions of the rat brain and inhibition by RS-8359. *Japanese journal of pharmacology* **1991,** *55* (1), 121-8.
17. Sader-Mazbar, O.; Loboda, Y.; Rabey, M. J.; Finberg, J. P., Increased L-DOPA-derived dopamine following selective MAO-A or -B inhibition in rat striatum depleted of dopaminergic and serotonergic innervation. *British journal of pharmacology* **2013,** *170* (5), 999-1013.

18. Wachtel, S. R.; Abercrombie, E. D., L-3,4-dihydroxyphenylalanine-induced dopamine release in the striatum of intact and 6-hydroxydopamine-treated rats: differential effects of monoamine oxidase A and B inhibitors. *Journal of neurochemistry* **1994,** *63* (1), 108-17.
19. Saura, J.; Bleuel, Z.; Ulrich, J.; Mendelowitsch, A.; Chen, K.; Shih, J. C.; Malherbe, P.; Da Prada, M.; Richards, J. G., Molecular neuroanatomy of human monoamine oxidases A and B revealed by quantitative enzyme radioautography and in situ hybridization histochemistry. *Neuroscience* **1996,** *70* (3), 755-74.
20. Saura, J.; Kettler, R.; Da Prada, M.; Richards, J. G., Quantitative enzyme radioautography with 3H-Ro 41-1049 and 3H-Ro 19-6327 in vitro: localization and abundance of MAO-A and MAO-B in rat CNS, peripheral organs, and human brain. *The Journal of neuroscience : the official journal of the Society for Neuroscience* **1992,** *12* (5), 1977-99.
21. Vitalis, T.; Fouquet, C.; Alvarez, C.; Seif, I.; Price, D.; Gaspar, P.; Cases, O., Developmental expression of monoamine oxidases A and B in the central and peripheral nervous systems of the mouse. *The Journal of comparative neurology* **2002,** *442* (4), 331-47.
22. Eisenhofer, G.; Kopin, I. J.; Goldstein, D. S., Catecholamine metabolism: a contemporary view with implications for physiology and medicine. *Pharmacological reviews* **2004,** *56* (3), 331-49.
23. De Deurwaerdere, P.; Di Giovanni, G.; Millan, M. J., Expanding the repertoire of L-DOPA's actions: A comprehensive review of its functional neurochemistry. *Progress in neurobiology* **2016**.
24. De Deurwaerdere, P.; Di Giovanni, G., Serotonergic modulation of the activity of mesencephalic dopaminergic systems: Therapeutic implications. *Progress in neurobiology* **2016**.
25. Fitoussi, A.; Dellu-Hagedorn, F.; De Deurwaerdere, P., Monoamines tissue content analysis reveals restricted and site-specific correlations in brain regions involved in cognition. *Neuroscience* **2013,** *255*, 233-45.
26. López-Gil, X.; Artigas, F.; Adell, A., Unraveling monoamine receptors involved in the action of typical and atypical antipsychotics on glutamatergic and serotonergic transmission in prefrontal cortex. *Current pharmaceutical design* **2010,** *16* (5), 502-15.
27. Copeland, R., *Enzymes: a practical introduction to structure, mechanism and data analysis.* second ed.; Wiley-VCH, Inc: New York, 2000.
28. Kitz, R.; Wilson, I. B., Esters of methanesulfonic acid as irreversible inhibitors of acetylcholinesterase. *The Journal of biological chemistry* **1962,** *237*, 3245-9.
29. De Colibus, L.; Li, M.; Binda, C.; Lustig, A.; Edmondson, D. E.; Mattevi, A., Three-dimensional structure of human monoamine oxidase A (MAO A): relation to the structures of rat MAO A and human MAO B. *Proceedings of the National Academy of Sciences of the United States of America* **2005,** *102* (36), 12684-9.
30. Esteban, G.; Allan, J.; Samadi, A.; Mattevi, A.; Unzeta, M.; Marco-Contelles, J.; Binda, C.; Ramsay, R. R., Kinetic and structural analysis of the irreversible inhibition of human monoamine oxidases by ASS234, a multi-target compound designed for use in Alzheimer's disease. *Biochimica et biophysica acta* **2014,** *1844* (6), 1104-10.
31. Cruciani, G.; Baroni, M.; Benedetti, P.; Goracci, L.; Fortuna, C. G., Exposition and reactivity optimization to predict sites of metabolism in chemicals. *Drug discovery today. Technologies* **2013,** *10* (1), e155-65.
32. Navailles, S.; Milan, L.; Khalki, H.; Di Giovanni, G.; Lagiere, M.; De Deurwaerdere, P., Noradrenergic terminals regulate L-DOPA-derived dopamine extracellular levels in a region-dependent manner in Parkinsonian rats. *CNS neuroscience & therapeutics* **2014,** *20* (7), 671-8.
33. Paxinos, G.; Watson, C., *The rat brain in stereotaxic coordinates*. Academic Press: San Diego, 1998.
34. De Deurwaerdere, P.; Bonhomme, N.; Le Moal, M.; Spampinato, U., d-fenfluramine increases striatal extracellular dopamine in vivo independently of serotonergic terminals or dopamine uptake sites. *Journal of neurochemistry* **1995,** *65* (3), 1100-8.
35. Tan, A. K.; Ramsay, R. R., Substrate-specific enhancement of the oxidative half-reaction of monoamine oxidase. *Biochemistry* **1993,** *32* (9), 2137-43.

36. Leslie, A. G., Integration of macromolecular diffraction data. *Acta crystallographica. Section D, Biological crystallography* **1999,** *55* (Pt 10), 1696-702.
37. Bailey, S., The CCP4 suite - Programs for prtein crystallography. *Acta crystallographica. Section D, Biological crystallography* **1994,** *55*, 760-763.
38. Emsley, P.; Lohkamp, B.; Scott, W. G.; Cowtan, K., Features and development of Coot. *Acta crystallographica. Section D, Biological crystallography* **2010,** *66* (Pt 4), 486-501.
39. Murshudov, G. N.; Skubak, P.; Lebedev, A. A.; Pannu, N. S.; Steiner, R. A.; Nicholls, R. A.; Winn, M. D.; Long, F.; Vagin, A. A., REFMAC5 for the refinement of macromolecular crystal structures. *Acta crystallographica. Section D, Biological crystallography* **2011,** *67* (Pt 4), 355-67.
40. McNicholas, S.; Potterton, E.; Wilson, K. S.; Noble, M. E., Presenting your structures: the CCP4mg molecular-graphics software. *Acta crystallographica. Section D, Biological crystallography* **2011,** *67* (Pt 4), 386-94.
41. D'Elia, P.; De Matteis, F.; Dragoni, S.; Shah, A.; Sgaragli, G.; Valoti, M., DP7, a novel dihydropyridine multidrug resistance reverter, shows only weak inhibitory activity on human CYP3A enzyme(s). *European journal of pharmacology* **2009,** *614* (1-3), 7-13.
42. Strano-Rossi, S.; Anzillotti, L.; Dragoni, S.; Pellegrino, R. M.; Goracci, L.; Pascali, V. L.; Cruciani, G., Metabolism of JWH-015, JWH-098, JWH-251, and JWH-307 in silico and in vitro: a pilot study for the detection of unknown synthetic cannabinoids metabolites. *Analytical and bioanalytical chemistry* **2014,** *406* (15), 3621-36.
43. Baranczewski, P.; Stanczak, A.; Sundberg, K.; Svensson, R.; Wallin, A.; Jansson, J.; Garberg, P.; Postlind, H., Introduction to in vitro estimation of metabolic stability and drug interactions of new chemical entities in drug discovery and development. *Pharmacological reports : PR* **2006,** *58* (4), 453-72.

Figure captions

Figure 1. Structure of *N*-(furan-2-ylmethyl)-*N*-methylprop-2-yn-1-amine (F2MPA), L-deprenyl and clorgyline.

Figure 2. Time course of the effect of clorgyline (left panel) or F2MPA (right panel) on basal and 3-MT-stimulated extracellular levels of HVA in the striatum. The MAOIs or their vehicle (sterile saline) were administered at 1 mg/kg intraperitoneally at the time corresponding to the arrow. 3-MT, dissolved in aCSF, was applied at 1, 10 and 100 µM for one hour at each concentration as indicated by the horizontal bars (white, 1 µM; grey 10 µM; black, 100 µM). Controls rats received aCSF only. Basal levels of HVA did not differ between groups before the administration of drugs and reached 3 ± 0.8 ng/30µl (n=20, 5 animals per group in the clorgyline experiment) or 2.6 ± 0.7 ng/30µl (n=19, 4 to 5 animals per group in the F2MPA experiment). Clorgyline significantly reduced the increase in HVA extracellular levels induced by 3-MT; *$p<0.05$ versus aCSF/saline group; °$p<0.05$ versus 3MT/clorgyline group, PLSD test after significant two-way ANOVA for each time point of the time course of effect.

Figure 3. Crystal structure of hMAO B in complex with F2MPA. (A) Zoomed-view ribbon representation (white) of hMAO B active site showing the covalent adduct formed by F2MPA (lawn green) with the enzyme flavin cofactor (yellow). Nitrogen, oxygen and phosphor atoms are blue, red and magenta, respectively. The unbiased $2F_o$-F_c electron density map for the F2MPA-flavin adduct contoured at 1.2 σ is colored in blue. It is important to note that some ambiguity exists in the position of the furan ring oxygen (see text) (B) hMAO B active site residues (carbon atoms in white) lining the enzyme cavity occupied by F2MPA. Color code is as in Figure 2A and water molecules are represented as red spheres. Hydrogen bonds are drawn as dashed lines. The inhibitor-flavin adduct is superposed to that formed by pargyline (PDB code 1GOS) represented with carbon atoms in brown. (C) Superposition of the MAO B-deprenyl adduct (PDB code 2BYB) onto that formed by F2MPA. Color code is as in Figure 2B.

Figure 4. CYP-dependent metabolic depletion of 10 μM F2MPA in human (■) and rat (●) liver microsomal preparations. Results are presented graphically in ln of percentage of compound recovery (100% at time 0 min) as a function of incubation time. Data are presented as mean ± s.e.m, of three different experiments.

Table 1. Effect of the systemic injection of MAOIs on the tissue content of DA, NE, 5-HT and metabolites in the striatum, the cortex and the hippocampus of rats.

	DA	DOPAC	HVA	NE	5-HT	5-HIAA
STRIATUM						
vehicle	2890 ± 341	813 ± 110	709 ± 90	232 ± 42	201 ± 32	346 ± 76
Clor. 1	3163 ± 610	434 ± 84*	535 ± 100	206 ± 33	205 ± 47	429 ± 104
Clor. 4	7273 ± 1702*	386 ± 92*	438 ± 66	148 ± 14	305 ± 75	267 ± 51
ANOVA	$F_{2,18}$= 4.2 #	$F_{2,18}$= 2.7 #	$F_{2,18}$= 1.1	$F_{2,18}$= 0.5	$F_{2,18}$= 0.6	$F_{2,18}$= 0.9
Depr. 1	4160 ± 501	955 ± 85	772 ± 77	191 ± 33	124 ± 24	329 ± 63
Depr. 4	2895 ± 605	697 ± 102	678 ± 92	167 ± 25	169 ± 25	406 ± 55
ANOVA	$F_{2,18}$= 1	$F_{2,18}$= 0.6	$F_{2,18}$= 0.7	$F_{2,18}$= 0.7	$F_{2,18}$= 1.8	$F_{2,18}$= 0.4
vehicle	3457 ± 163	822 ± 8	666 ± 35	235 ± 11	355 ± 4	243 ± 10
F2MPA 1	2669 ± 143*	829 ± 15	664 ± 39	239 ± 10	162 ± 14*	172 ± 11*
F2MPA 4	3651 ± 84	859 ± 14	846 ± 17	258 ± 16	241 ± 18*	252 ± 10
ANOVA	$F_{2,15}$= 15 #	$F_{2,15}$= 2.2	$F_{2,15}$= 9.9 #	$F_{2,15}$= 0.9	$F_{2,15}$= 52 #	$F_{2,15}$= 19 #
CORTEX						
vehicle	10 ± 1	50 ± 7	nd	359 ± 94	362 ± 27	278 ± 47
Clor. 1	11 ± 3	47 ± 10		170 ± 29	567 ± 14	202 ± 29
Clor. 4	14 ± 4	43 ± 5		228 ± 40	819 ± 13*	184 ± 27
ANOVA	$F_{2,18}$= 0.4	$F_{2,18}$= 0.2	nd	$F_{2,18}$= 2.3	$F_{2,18}$= 4 #	$F_{2,18}$= 2
Depr. 1	13 ± 2	58 ± 9		195 ± 44	364 ± 21	464 ± 178
Depr. 4	48 ± 30	74 ± 16		257 ± 28	495 ± 41*	384 ± 89
ANOVA	$F_{2,18}$= 3.1	$F_{2,18}$= 1.2		$F_{2,18}$= 1.6	$F_{2,18}$= 4.5 #	$F_{2,18}$= 0.5
vehicle	nd	nd	nd	356 ± 16	262 ± 10	323 ± 12
F2MPA 1				547 ± 14*	484 ± 21*	405 ± 6*
F2MPA 4				633 ± 9*	243 ± 6	478 ± 13*
ANOVA				$F_{2,15}$= 108 #	$F_{2,15}$= 340 #	$F_{2,15}$= 18 #
HIPPOCAMPUS						
vehicle	nd	nd	nd	390 ± 67	161 ± 34	409 ± 57
Clor. 1				418 ± 95	241 ± 51	237 ± 57 *
Clor. 4				260 ± 55	284 ± 96	180 ± 35 *
ANOVA				$F_{2,18}$= 1.2	$F_{2,17}$= 0.9	$F_{2,18}$= 5.6 #
Depr. 1				554 ± 74	139 ± 30	366 ± 52
Depr. 4				430 ± 109	140 ± 38	354 ± 75
ANOVA				$F_{2,18}$= 1.3	$F_{2,17}$= 0.2	$F_{2,18}$= 0.8
vehicle	nd	nd	nd	508 ± 43	177 ± 9	420 ± 79
F2MPA 1				512 ± 34	239 ± 24	417 ± 26
F2MPA 4				505 ± 51	266 ± 65	306 ± 61
ANOVA				$F_{2,15}$= 0.01	$F_{2,15}$= 1.3	$F_{2,15}$= 1.3

Results are expressed in picograms/mg of tissue in the striatum, the cortex and the hippocampus. Clor. and Depr. correspond to clorgyline and deprenyl, respectively. 1 and 4 indicate the dose in mg/kg. nd, not detected; *p<0.05, (PLSD test). The results of the one-way ANOVA has been given below each experimental group together with the indication of its significance (#p<0.05). The vehicle group (n=7) was identical for clorgyline (n= 7 for both doses) and deprenyl (n=7 for both doses) experiments. The F2MPA experiment at 1 (n=6) or 4 (n=5) mg/kg was performed separately with its own vehicle group (n= 5).

Table 2. Kinetic parameters for inactivation of MAO at 30°C by propargyl compounds.

Enzyme	Parameter	FMPA	Clorgyline	Deprenyl
IC_{50} (30 min)				
hMAO A	IC_{50}	232 ± 15 μM	0.23 ± 0.05 nM	17.0 ± 0.4 μM
hMAO B	IC_{50}	8.9 ± 1.2 μM	10.6 ± 0.95 μM	12.6 ± 1.1 nM
Rat MAO[a]				
MAO A	IC_{50}	121 ± 55 μM	1.81 ± 0.60 nM	17.6 ± 6.7 μM
MAO B	IC_{50}	4.15 ± 0.42 μM	4.2 ± 1.2 μM	7.8 ± 1.1 nM
Inactivation				
hMAO A	k_{inact} (min^{-1})	0.087 ± 0.010	0.157 ± 0.018*	0.252 ± 0.081
	K_I (μM)	187 ± 37	0.031 ± 0.009*	193 ± 55
	k_{inact}/K_I	**0.0005**	**5.06**	**0.0013**
hMAO B	k_{inact} (min^{-1})	0.61 ± 0.09	0.020 ± 0.001	1.06 ± 0.25
	K_I (μM)	135 ± 23	1.8 ± 0.6	0.18 ± 0.05
	k_{inact}/K_I	**0.0045**	**0.10**	**5.89**
Rat MAO B[b]	k_{inact} (min^{-1})	0.53 ± 0.03		
	K_I (μM)	65 ± 7		
	k_{inact}/K_I	**0.0082**		

[a]All three inhibitors gave biphasic dose-response curves for rat MAO inactivation. The smaller fraction (34%) is identified as MAO A by the high affinity clorgyline inhibition; the larger fraction (66%) inhibited at high affinity by deprenyl is identified as MAO B.

[b]Rat liver homogenate was pre-treated with clorgyline to block MAO A.

Table 3. Data collection and refinement statistics for the human MAO B-F2MPA complex

PDB code	XXXX
Space group	C222
Unit cell axes (Å)	*a* = 131.8, *b* = 223.2, *c* = 86.5
Resolution (Å)	2.4
R_{sym} [a,b] (%)	16.5 (75.1)
$CC_{1/2}$ (%)	99.0 (78.1)
Completeness[b] (%)	98.4 (95.4)
Unique reflections	48,068
Redundancy	7.7 (6.7)
I/σ[b]	9.9 (4.0)
N° of atoms	
protein/FAD/ligand/water	7915/2x53/2x11/223
Average B value for	
ligand atoms (Å^2)	48.3
R_{cryst} [b,c] (%)	17.0 (23.2)
R_{free} [b,c] (%)	23.7 (31.3)
Rms bond length (Å)	0.016
Rms bond angles (°)	1.76

[a] $R_{sym}=\sum|I_i-<I>|/\sum I_i$, where I_i is the intensity of i^{th} observation and <I> is the mean intensity of the reflection.

[b] Values in parentheses are for reflections in the highest resolution shell.

[c] $R_{cryst}=\sum|F_{obs}-F_{calc}|/\sum|F_{obs}|$ where F_{obs} and F_{calc} are the observed and calculated structure factor amplitudes, respectively. R_{cryst} and R_{free} were calculated using the working and test sets, respectively.

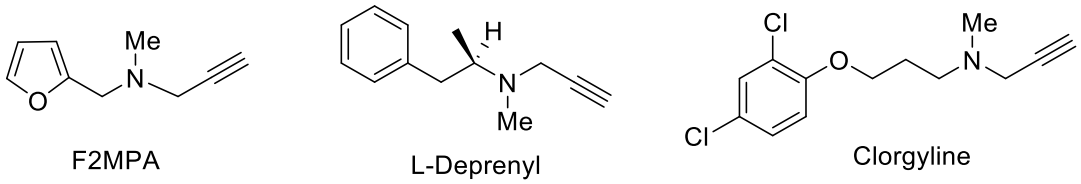

Figure 1

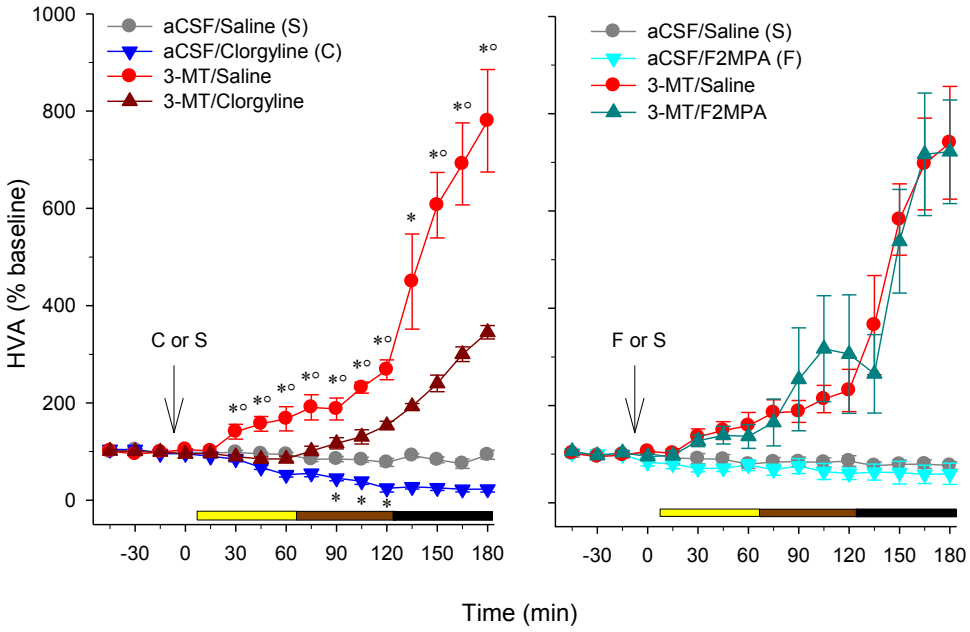
aCSF/Saline (S)
aCSF/Clorgyline (C)
3-MT/Saline
3-MT/Clorgyline
aCSF/Saline (S)
aCSF/F2MPA (F)
3-MT/Saline
3-MT/F2MPA
HVA (% baseline)
C or S
F or S
Time (min)
1000
800
600
400
200
0
-30
0
30
60
90
120
150
180

Figure 2

A.

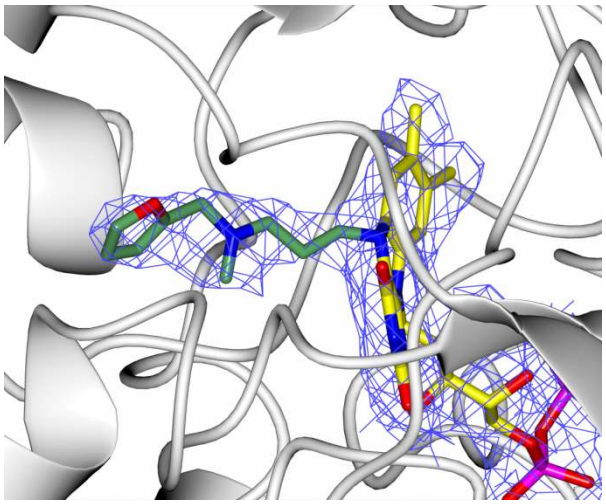

B.

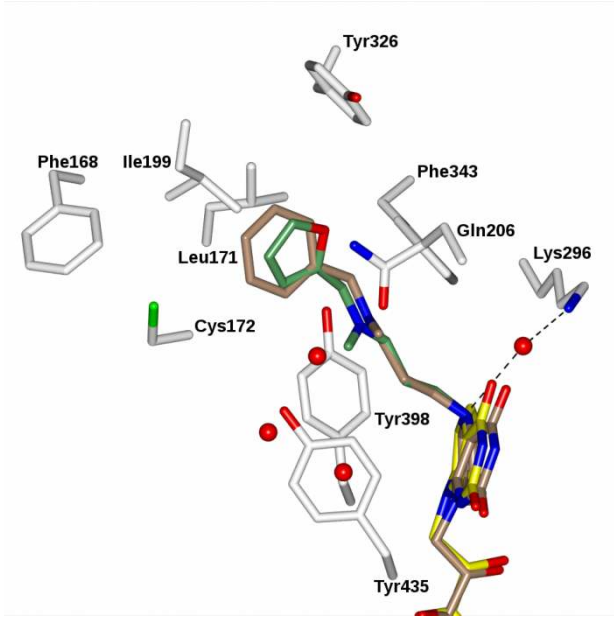
Tyr326
Phe168
Ile199
Phe343
Gln206
Leu171
Lys296
Cys172
Tyr398
Tyr435

C.

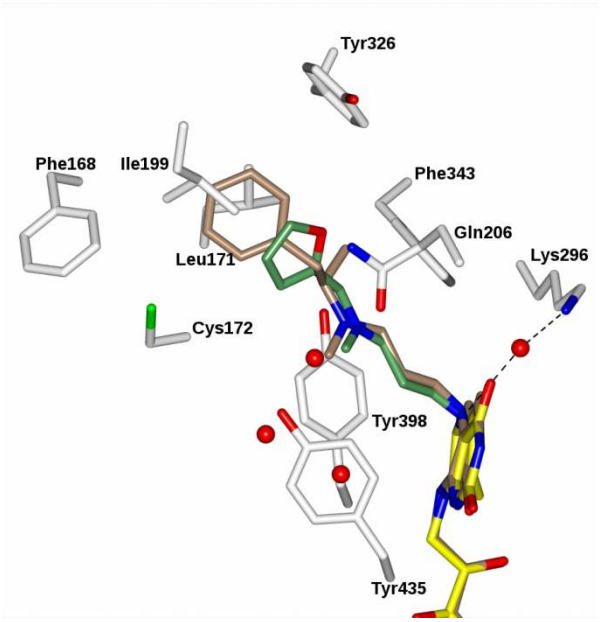
Tyr326
Phe168
Ile199
Phe343
Gln206
Leu171
Lys296
Cys172
Tyr398
Tyr435

Figure 3

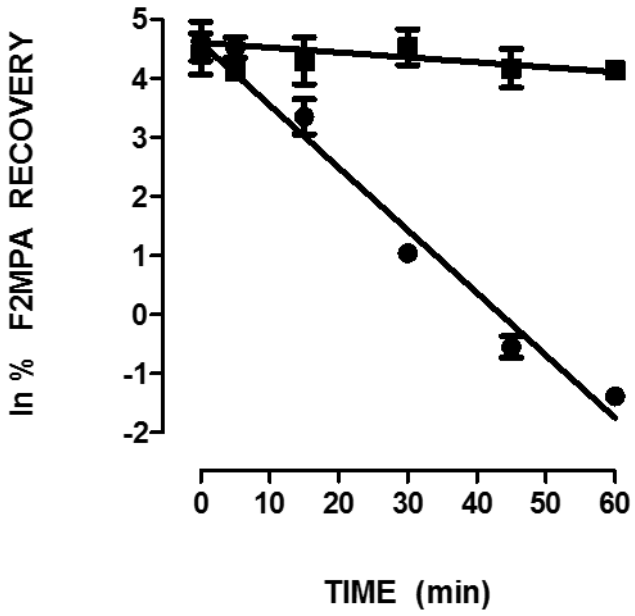

Figure 4